Research Article

Pulmonary Circulation

Rare variants in *RNF213*, a susceptibility gene for moyamoya disease, are found in patients with pulmonary hypertension and aggravate hypoxia-induced pulmonary hypertension in mice

Hatasu Kobayashi[1,2,*], Risako Kabata[1,*], Hideyuki Kinoshita[3], Takaaki Morimoto[1,4], Koh Ono[3], Midori Takeda[1], Jungmi Choi[1], Hiroko Okuda[1], Wanyang Liu[5], Kouji H. Harada[1], Takeshi Kimura[3], Shohab Youssefian[6] and Akio Koizumi[1]

[1]Department of Health and Environmental Science, Graduate School of Medicine, Kyoto University, Kyoto, Japan; [2]Department of Biomedical Sciences, College of Life and Health Sciences, Chubu University, Kasugai, Japan; [3]Department of Cardiovascular Medicine, Graduate School of Medicine, Kyoto University, Kyoto, Japan; [4]Department of Neurosurgery, Graduate School of Medicine, Kyoto University, Kyoto, Japan; [5]Department of Nutrition and Food Hygiene, School of Public Health, China Medical University, Shenyang, People's Republic of China; [6]Laboratory of Molecular Biosciences, Graduate School of Medicine, Kyoto University, Kyoto, Japan

Abstract

Ring finger 213 (*RNF213*) is a susceptibility gene for moyamoya disease (MMD), a progressive cerebrovascular disease. Recent studies suggest that *RNF213* plays an important role not only in MMD, but also in extracranial vascular diseases, such as pulmonary hypertension (PH). In this study, we undertook genetic screening of *RNF213* in patients with PH and performed functional analysis of an *RNF213* variant using mouse models. Direct sequencing of the exons in the C-terminal region of *RNF213*, where MMD-associated mutations are highly clustered, and of the entire coding exons of *BMPR2* and *CAV1*, the causative genes for PH, was performed in 27 Japanese patients with PH. Two MMD-associated rare variants (p.R4810K and p.A4399T) in *RNF213* were identified in two patients, three *BMPR2* mutations (p.Q92H, p.L198Rfs*4, and p.S930X) were found in three patients, whereas no *CAV1* mutations were identified. To test the effect of the *RNF213* variants on PH, vascular endothelial cell (EC)-specific *Rnf213* mutant transgenic mice were exposed to hypoxia. Overexpression of the EC-specific *Rnf213* mutant, but neither *Rnf213* ablation nor EC-specific wild-type *Rnf213* overexpression, aggravated the hypoxia-induced PH phenotype (high right ventricular pressure, right ventricular hypertrophy, and muscularization of pulmonary vessels). Under hypoxia, electron microscopy showed unique EC detachment in pulmonary vessels, and western blots demonstrated a significant reduction in caveolin-1 (encoded by *CAV1*), a key molecule involved in EC functions, in lungs of EC-specific *Rnf213* mutant transgenic mice, suggestive of EC dysfunction. *RNF213* appears to be a genetic risk factor for PH and could play a role in systemic vasculopathy.

Keywords

genetics, genomics, epigenetics, animal models, endothelium, caveolin-1

Date received: 16 December 2017; accepted: 30 April 2018

Pulmonary Circulation 2011; 8(3) 1–13
DOI: 10.1177/2045894018778155

Ring finger 213 (*RNF213*)/mysterin was recently identified as a susceptibility gene for moyamoya disease (MMD).[1,2] In addition, the p.R4810K variant of *RNF213* (rs112735431) was determined as a founder polymorphism that is strongly associated with MMD in East Asian populations.[1,2] MMD is an uncommon, chronic progressive cerebrovascular

*Equal contributors.

Corresponding author:
Hideyuki Kinoshita, Department of Cardiovascular Medicine, Graduate School of Medicine, Kyoto University, Konoe-cho, Yoshida, Sakyo-ku, Kyoto 606-8501, Japan.
Email: kinos@kuhp.kyoto-u.ac.jp

disease characterized by stenosis/occlusion of the arteries around the circle of Willis with prominent arterial collateral circulation that resembles a puff of smoke, or moyamoya in Japanese.[3–5]

An early histopathological report showed not only intracranial but also extracranial vascular changes in patients with MMD.[6] We recently reported that the *RNF213* p.R4810K variant was significantly associated with coronary artery disease in the Japanese population.[7] Our group also demonstrated a significant association of *RNF213* p.R4810K with systolic blood pressure.[8] These findings suggested that *RNF213* plays an important role in the etiology of other vascular diseases besides MMD.

Pulmonary hypertension (PH) is a severe progressive disease, resulting in elevated pulmonary arterial pressure (PAP), vascular remodeling, and right ventricular heart failure.[9] The exact etiology of PH remains largely unknown. However, genetic risk factors, such as mutations in bone morphogenic protein receptor type 2 (*BMPR2*), the most common causative gene of PH,[10,11] play an important role in PH:[12] about 80% of patients with a family history of PH and about 25% of those with sporadic cases.[13] A prominent feature of the molecular pathology of PH related to *BMPR2* is vascular endothelial cell (EC) dysfunction, characterized by the hallmark phenotype such as reduced angiogenesis.[14] It is interesting that loss of function mutations in the *CAV1* gene, which encodes caveolin-1 (Cav-1), have also been reported in *BMPR2* mutation negative patients, and that ablation of Cav-1 promotes PH.[15–17] Furthermore, recent data have clarified the relationship between *BMPR2* mutations and caveolar trafficking defects in vascular EC dysfunction.[18] These data collectively indicate that *BMPR2* mutations cause PH through a decrease in Cav-1 signaling via reduced angiogenesis.

Nine cases with co-occurrence of PH and MMD have been reported in five studies,[19–23] two of which[19,23] interestingly reported that patients with concurrent PH and MMD carried homozygous *RNF213* p.R4810K, suggesting that *RNF213* may be a risk factor common to both MMD and PH.

RNF213, which was first cloned and characterized by our group,[1] encodes a large protein composed of 5207 amino acids with a molecular weight of 591 kDa that is ubiquitously expressed. Morito et al.[24] demonstrated that *RNF213* has two AAA+ domains (D1, D2) that form a hexameric ring. The ATP binding site of the Walker A motif of the D1 initiates oligomerization, whereas ATP hydrolysis by the D2 causes dissociation of the oligomeric structure. In addition, *RNF213* has a ring finger domain that functions as an E3 ligase.[1] *RNF213* has 69 exons, of which exon 4 is skipped in most tissues, including the vascular system.[1] The reported variants associated with MMD are mostly missense variants that are exclusively located in the C-terminal region of the ring finger domain (i.e. exon 43),[25] suggesting a crucial role of mutations in the ring finger region in the pathology of MMD.

With regard to the molecular functions of *RNF213*, various lines of evidence suggest that *RNF213* is involved in important signal cascades, such as Wnt signaling,[26] the protein-tyrosine phosphatase-1B (PTP1B) pathway,[27] as well as inflammation.[28,29] In vitro analysis has shown that ECs, differentiated from iPS cells established from patients carrying *RNF213* p.R4810K, displayed reduced angiogenesis.[30] Similarly, overexpression of *RNF213* p.R4810K by transfection of cultured human ECs, as well as induction of *RNF213* p.R4810K by interferon treatment, have also been shown to result in reduced angiogenesis.[29] Transgenic mice overexpressing *Rnf213* p.R4757K (human ortholog of p.R4810K) specifically in ECs exposed to hypoxia show reduced angiogenesis, whereas mice overexpressing *Rnf213* p.R4757K in vascular smooth muscle cells (SMCs), or those overexpressing wild-type (WT) *Rnf213* in ECs, or mice in which *Rnf213* had been ablated did not inhibit such adaptive angiogenesis after hypoxia.[29] Several case reports[19–23] of PH and MMD co-morbidity collectively suggest that, through cross-talk with *BMPR2* in cascades such as inflammation or Wnt signaling, *RNF213* may also be a susceptible gene for PH. We were, therefore, tempted to speculate that specific mutations in *RNF213* may lead to EC dysfunction and thereby impaired hypoxia-induced adaptive angiogenesis, which underlies the pathology of both MMD and PH.

In the current study, we tested this hypothesis by first screening 27 patients with PH for rare *RNF213* variants, as well as for variants in major genes associated with PH, such as *BMPR2*, *CAV1*, *ACVRL1*, and *ENG*.[31] As the small number of patients precluded the possibility of statistically analyzing the aggregation of deleterious *RNF213* mutations, we examined the effects of the *Rnf213* p.R4757K variant on the PH phenotype using mouse models exposed to hypoxia. Of the various lines of mice that we created, only those with EC-specific expression of *RNF213* p.R4757K showed a significantly exaggerated PH phenotype, whereas those overexpressing WT *Rnf213* or those in which *Rnf213* was ablated displayed no such phenotype.

Methods

Ethics statement

This study was conducted in accordance with the Declaration of Helsinki standards and was approved by the ethics committee of Kyoto University (approval no. G342; approval date 25 December 2009). Written informed consent was obtained from all participants or their parents if they were aged < 20 years.

Care of animals and all experimental procedures were in accordance with the Animal Welfare Guidelines of Kyoto University. The experimental protocol was authorized by the Internal Animal Welfare Committee at Kyoto University (approval no. Med Kyo17051; approval date 27 March 2017).

Table 1. Demographic characteristics and PH classifications.

Total (n)		27
Age at diagnosis (years), mean (±SD)		52.6 ± 22.2
Male sex (n (%))		10 (37.0)
Clinical subtype of PH[9] (n (%))	Group 1 (PAH)	17 (63.0)
	Idiopathic PAH (IPAH)	11
	Heritable PAH	0
	Associated with connective tissue disease	4
	Associated with congenital heart disease	2
	Group 2 (PH due to left heart disease)	1 (3.7)
	Group 3 (PH due to lung diseases and/or hypoxia)	4 (14.8)
	Group 4 (chronic thromboembolic PH)	5 (18.5)
	Group 5 (PH due to unclear multifactorial mechanisms)	0 (0)

Patients and clinical characterization

We performed a case series study of 30 Japanese patients, without a blood relationship, that were admitted to the cardiology division of Kyoto University Hospital with the diagnosis of PH between April 2010 and August 2013. Of these, three patients were excluded because of poor DNA quality and 27 patients were ultimately enrolled. Before genetic analysis, the diagnosis of PH subtype (group 1, pulmonary arterial hypertension (PAH); group 2, PH due to left heart disease; group 3, PH due to lung diseases and/or hypoxia; group 4, chronic thromboembolic PH; group 5, PH due to unclear multifactorial mechanisms; Table 1) was made according to international recommendations.[9] Serum samples for DNA extraction were collected at the first admission.

We collected the following information from medical records written at diagnosis: demographic characteristics (age and sex); pulmonary function parameters (forced vital capacity, forced expiratory flow in 1 s, and carbon monoxide diffusing capacity); and hemodynamic variables (mean right atrial pressure, mean PAP, pulmonary vascular resistance (PVR), and the cardiac index).

*Sequencing of **RNF213**, **BMPR2**, **CAV1**, **ACVRL1**, and **ENG** genes*

Genomic DNA was obtained from peripheral blood serum samples using the DNA Blood Mini Kit (Qiagen, Hilden, Germany). Sanger sequencing was performed using the Big Dye Terminator V1.1 cycle sequencing kit with an ABI PRISM 3130 genetic analyzer (Thermo Fisher Scientific, Waltham, MA, USA). For *RNF213,* exons 41–69 (based on RefSeq no. NM_020914.4) and their intron/exon boundaries, which correspond to its C-terminal region where the MMD-associated mutations are highly clustered,[25] were sequenced in all study subjects. Primer sequences were as described previously.[1] We also sequenced the entire coding region and intron/exon boundaries of the *BMPR2* gene (exons 1–13 based on RefSeq no. NM_001204.6, primer sequences shown in Table S1) and the *CAV1* gene (exons 1–3 based on RefSeq no. NM_001753.4, primer sequences shown in Table S2). The sample from one patient with concurrent hereditary hemorrhagic telangiectasia (HHT) was also used for sequence analysis of the entire coding region and intron/exon boundaries of two known HHT causative genes;[32] *ACVRL1* (exons 2–10 based on RefSeq no. NM_000020.2, primer sequences shown in Table S3), and *ENG* (exons 1–14 based on RefSeq no. NM_000118.3, primer sequences described previously[33]). The identified variants were sequenced with both forward and reverse primers.

Database search for variants

The effect of the variants on protein function was assessed using two in silico prediction algorithms: PolyPhen2 (http://genetics.bwh.harvard.edu/pph2) and SIFT (http://sift.bii.a-star.edu.sg/). The 1000 Genomes Project (http://www.1000genomes.org/) was used to investigate the frequency of each variant in the Japanese population. We filtered for variants, based on minor allele frequencies (MAF) from the 1000 Genomes JPT, and previous publications related to MMD or PH. Variants with MAF > 1% were filtered out unless there was evidence of an association with MMD or PH for such variants. A variant was included if there was evidence that it was associated with MMD or PH.

Generation of mice and hypoxic exposure

Vascular EC-specific *Rnf213* WT and R4757K (mutation corresponding to human *RNF213* R4810K) transgenic (Tg) mice (EC-WT Tg and EC-Mut Tg mice, respectively)[29] and global *Rnf213* knockout mice (KO mice)[34] were generated in a C57BL/6 background as previously described. Briefly, we generated founder Tg mice using the transgene construct harboring the loxP-flanked transcription termination sequence (beta globin poly(A)) between the CAG promoter and mouse *Rnf213* (WT or R4757K mutant) coding sequence. To obtain mice harboring vascular EC-overexpressing *Rnf213*, founder Tg mice were bred

with mice expressing Tie2-Cre as previously reported.[29] *Rnf213* KO mice were produced by deletion of *Rnf213* exon 20 using targeted recombination and the Cre-/loxP approach.

Hypoxia experiments were performed in four groups of mice aged 8–10 weeks as follows: (1) EC-Mut Tg; (2) EC-WT Tg; (3) KO; and (4) WT C57BL/6 mice. Mice were exposed to hypoxia by placing them in a 10% oxygen chamber with nitrogen-balanced gas under normal atmospheric pressure (Kyodo International, Kanagawa, Japan) for one or four weeks.[35] EC-Mut Tg and WT mice were also kept under 10% oxygen for 12 weeks.

Physiological assessment of PH mouse models

Thoracotomy was performed under positive pressure ventilation and general anesthesia with isoflurane. Right ventricular systolic pressure (RVP) was measured by inserting a catheter directly into the right ventricle. After RVP measurement, mice were sacrificed, and the lungs and heart were collected. To evaluate right ventricular hypertrophy, the ratio of right ventricular weight to left ventricular and septal weight (RV/(LV + S)) was determined.

Pathological analysis

To evaluate pathological changes in pulmonary arteries, immunohistochemistry for alpha smooth muscle actin (αSMA) and electron microscopy were performed using collected mouse lungs. Immunohistochemistry was also performed to examine Cav-1 protein expression in pulmonary vascular ECs. For immunohistochemistry, lungs were fixed in 10% formaldehyde, embedded in paraffin, and sectioned. The sections were immunostained with mouse anti-αSMA (Sigma-Aldrich, St. Louis, MO, USA) or anti-Cav-1 (Cell Signaling Technology, Beverly, MA, USA) antibodies, followed by incubation with biotinylated anti-mouse IgG or anti-rabbit IgG (Vector Labs, Burlingame, CA, USA). Detection was performed by ABC/DAB immunohistochemistry using the ABC kit (Vectastain; Vector Labs). To quantitate αSMA immunostaining, the number and thickness of αSMA-positive vessels were measured in five high-power fields (including 10–15 αSMA (+) vessels) per mouse using Image-J software (National Institutes of Health). Vessel thickness was divided by vascular diameter to adjust for variation in vessel size. For electron microscopy, lungs were fixed in 2% glutaraldehyde and post-fixed in 1% osmium tetroxide. The samples were dehydrated through a graded ethanol series, embedded in Epon, sectioned with an ultramicrotome (EM UC6; Leica, Wetzlar, Germany), and stained with lead citrate. Sections were observed by transmission electron microscopy (H-7650; Hitachi, Tokyo, Japan).

Histological analysis of the mouse brain was also performed to evaluate cerebral blood vessels. Hypoxia-induced cerebral angiogenesis was examined by immunohistochemistry for glucose transporter (GLUT)-1 as previously described.[29] The thickness of cerebral blood vessels was assessed using H&E-stained sections. Vessel thickness was divided by the vascular diameter to adjust for variation of vessel size. Quantification was performed on five high-power fields per mouse by Image-J software.

Western blotting

Mouse lungs were lysed in CelLytic MT Cell Lysis Reagent (Sigma-Aldrich) containing a protease inhibitor cocktail (Nacalai Tesque, Kyoto, Japan). Lysates were separated by SDS-PAGE and transferred onto polyvinylidene fluoride membranes by standard procedures. After blocking, membranes were incubated with primary antibodies against Cav-1 (Cell Signaling Technology) or β-actin (Cell Signaling Technology), and subsequently with peroxidase-conjugated anti-rabbit IgG secondary antibody (Sigma-Aldrich). Immunodetection was performed using ECL Prime detection reagent (GE Healthcare, Little Chalfont, UK) and scanning on a Fujifilm LAS-3000 system. Quantification was performed using Image Studio software (LI-COR Biosciences, Lincoln, NE, USA).

Statistical analysis

Demographic and clinical parameters are presented as mean ± standard deviation (SD). Results of the animal studies are presented as mean ± standard error of the mean (SEM). Differences among the means of mouse groups were evaluated using one-way ANOVA to avoid false positives by multiple comparisons. When one-way ANOVA was significant ($P < 0.05$), then Tukey's post-hoc test was conducted to detect different groups. Two-way ANOVA was also performed to assess effects of genotype, hypoxia and their interactions. When two groups were compared, Student's t-test was used. All statistical analyses were conducted using JMP software (SAS Institute, Cary, NC StatSoft, Tulsa, OK, USA). $P < 0.05$ was considered statistically significant.

Results

Clinical characteristics of the patients

Demographic characteristics and PH subtype classifications of the 27 patients in the present study are shown in Table 1. The mean age at diagnosis was 52.6 ± 22.2 (mean ± SD) years and the proportion of men was 37.0%. In the 27 patients with PH, 17 (63.0%) were diagnosed with PAH, including idiopathic PAH (IPAH) (n = 11), PAH associated with connective tissue disease (n = 4), and PAH associated with congenital heart disease (n = 2). There were no cases of heritable PAH. The other patients were classified as having PH due to left heart disease (3.7%, 1/27), PH due to lung diseases and/or hypoxia (14.8%, 4/27), or chronic thromboembolic PH (18.5%, 5/27).

*Identification of **RNF213** and BMPR2 variants in PH cases*

Among the 27 patients with PH, we found 14 variants including seven non-synonymous variants in *RNF213* and *BMPR2*, but no variants in *CAV1* (Table S4). Variants were also not identified in *ENG* or *ACVRL1* from one patient with PH and HHT (Table S4).

Of the total of ten *RNF213* variants, we found four non-synonymous variants (p.V3838L, p.E3915G, p.A4399T, and p.R4810K) in the sequenced region of three patients (Table S4). As a result of filtering, p.V3838L and p.E3915G were excluded because of an MAF > 1%, and the absence of evidence of an association with MMD.

Of the total of four *BMPR2* variants, three non-synonymous variants (p.Q92H, p.L198Rfs*4, and p.S930X) were observed in three patients (Table S4). These three variants were included after filtering because of an MAF < 1%, or a reported association with PH. The included *RNF213* and *BMPR2* variants were heterozygous, and none of the patients displayed co-existing *RNF213* and *BMPR2* variants (Table S4).

Cases of PH harboring *RNF213* variants

RNF213 p.A4399T and p.R4810K (Fig. S1A and B) were considered to be disease-causing as p.R4810K[1] and p.A4399T[36] have been associated with MMD. Further support for the pathological roles of these variants was obtained from the "Possibly Damaging" and "Intolerant" prediction outcomes by PolyPhen-2 and SIFT, respectively (Table 2). Interestingly, one patient with p.R4810K showed severe symptoms of PH (mean PAP = 74 mmHg; PVR = 18.3 [Wood units]; Table 3) and a poor prognosis. At the age of 45 years, this patient was diagnosed with IPAH, displayed rapid progression of PH and treatment resistance, and died only 16 months after diagnosis. High-resolution chest computed tomography (CT) of this patient showed neovascularity, as tiny and serpiginous intrapulmonary vessels in the periphery of the lungs and ground-glass

Table 2. Pathogenic variations in *RNF213* and *BMPR2*.

Gene	Variant	rs number (dbSNP149)	Polyphen-2	SIFT	MAF (%) in 1000 Genomes JPT	Reference
RNF213	p.A4399T	rs148731719	Possibly damaging	Intolerant	6.7	Wu et al., 2012[36]
RNF213	p.R4810K	rs112735431	Possibly damaging	Intolerant	1.0	Liu et al., 2011[1]
BMPR2	p.Q92H	rs140683387	Benign	Intolerant	1.4	Kabata et al., 2013[37]
BMPR2	p.L198Rfs*4	-	-	-	0.0	-
BMPR2	p.S930X	-	-	-	0.0	Morisaki et al., 2004[38]

Table 3. Clinical characteristics of patients with PH and *RNF213* or *BMPR2* variants.

	Total (n = 27) (mean ± SD)	*RNF213* p.A4399T	*RNF213* p.R4810K	*BMPR2* p.Q92H	*BMPR2* p.L198Rfs*4	*BMPR2* p. S930X
PH subtype	-	Group 3 (IP)	Group 1 (IPAH)	Group 1 (PSS)	Group 1 (IPAH)	Group 1 (IPAH)
Mean age at diagnosis (years)	52.6 ± 22.2	82	45	59	10	59
Sex	Male = 37.0%	Female	Female	Female	Female	Female
%FVC	83.6 ± 22.3	82.1	96.7	73.8	71.7	115.1
FEV1 (%(G))	77.6 ± 10.5	90.9	77.9	94.44	88.13	78.4
DLCO (%)	50.1 ± 18.9	NA	NA	40.7	57.1	NA
mRAP (mmHg)	6.50 ± 5.52	3	6	3	NA	10
mPAP (mmHg)	42.4 ± 14.7	31	74	19	NA	59
PVR (WU)	9.59 ± 7.46	3.26	18.3	3.09	NA	27.8
CI (L/m/m^2)	2.85 ± 1.04	3.31	2.28	3.45	NA	0.43

IP, interstitial pneumonia; IPAH, idiopathic pulmonary arterial hypertension; PSS, progressive systemic sclerosis; FVC, forced viral capacity; FEV1, forced expiratory volume in 1 s; DLCO, diffusing capacity of carbon monoxide; mPAP, mean pulmonary artery pressure; mRAP, mean right atrial pressure; PVR, pulmonary vascular resistance; CI, cardiac index; NA, not available.

opacity (GGO) within the lungs (Fig. 1a). Notably, p.A4399T was also found in patients with PH and interstitial pneumonia (Table 3), suggesting the involvement of inflammation.

Cases of PH harboring *BMPR2* variants

Three *BMPR2* non-synonymous variants were found in three (11.1%) patients. One novel frameshift mutation (c.593_594delTT, p.L198Rfs*4) (Fig. S1D) was identified in exon 5 of *BMPR2* in a patient with early-onset (at the age of 10 years) IPAH (Table 3). An axial CT scan with lung windows of this patient also showed neovascularity as tiny and serpiginous intrapulmonary vessels in the periphery of the lungs and GGO within the lungs (Fig. 1b). Two of these variants, p.Q92H and p.S930X (Fig. S1C and E), have been described in previous literature on PH.[37,38] P.Q92H was found in a patient with PH with progressive systemic sclerosis, while p.S930X was identified in a patient with IPAH (Table 3).

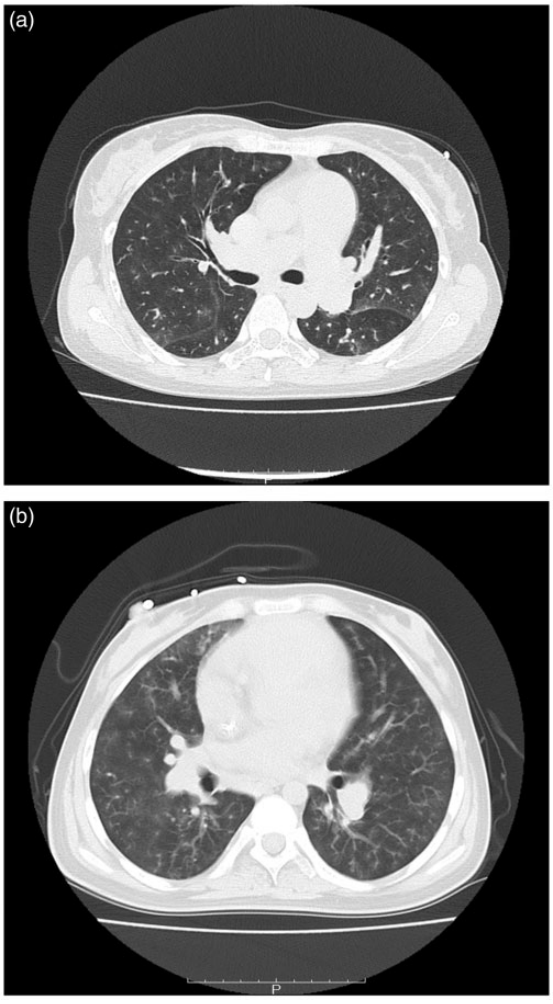

Fig. 1. CT scan data of PH patients with *RNF213* and *BMPR2* variants. (a) Axial CT scan with lung windows in a 45-year-old IPAH patient with RNF213 p.R4810K. Neovascularity, shown as tiny and serpiginous intrapulmonary vessels, can be seen in the periphery of the lungs and GGO is observed within the lungs. (b) Axial CT scan with lung windows in an IPAH patient with *BMPR2* p.L198Rfs*4. Neovascularity, shown as tiny and serpiginous intrapulmonary vessels, can also be seen in the periphery of the lungs and GGO appears within the lungs.

PH induced by hypoxia for four and 12 weeks

To investigate the effects of the identified *RNF213* variants (including p.R4810K) on PH, we evaluated several physiological parameters of PH in EC-Mut Tg, EC-WT Tg, KO, and WT mice under hypoxia. We used EC-specific Tg mouse models in the present study because our previous study[29] indicated that under hypoxia, EC-specific *Rnf213* mutant Tg mice, but not vascular SMC-specific *Rnf213* mutant Tg mice, displayed the hallmark of vascular phenotype, i.e. reduced angiogenesis. As expected, hypoxic exposure significantly elevated RVP and RV/(LV + S) in all genotypes of mice (Fig. 2), which confirmed the hypoxia-induced PH model. Notably, EC-Mut Tg mice exposed to hypoxia for four weeks showed significantly higher RVP and RV/(LV + S) than the EC-WT Tg, KO, and WT mice. However, the RVP and RV/(LV + S) did not differ between any of the mice genotypes under normoxia (Fig. 2). Additionally, two-way ANOVA indicates that the genotypes and hypoxia significantly affected RVP and RV/(LV + S), and that the interaction was significant (Fig. 2). These findings indicated that *Rnf213* mutant overexpression in ECs, but not *Rnf213* WT overexpression in ECs nor *Rnf213* ablation, aggravated the PH phenotype induced by hypoxic exposure. To determine whether longer-term exposure to hypoxia also leads to more severe aggravation by the *Rnf213* mutant, we evaluated the physiological parameters in EC-Mut Tg and WT mice exposed to hypoxia for 12 weeks. However, RVP (EC-Mut Tg: 4 weeks 54.3 mmHg vs 12 weeks 50.7 mmHg; WT: 4 weeks 41.3 mmHg vs 12 weeks 40.5 mmHg) and RV/(LV + S) (EC-Mut Tg: 4 weeks 0.397 vs 12 weeks 0.400; WT: 4 weeks 0.336 vs 12 weeks 0.354) in mice under hypoxia for 12 weeks were similar to those exposed to hypoxia for four weeks and were again significantly higher in the EC-Mut Tg than WT mice. (Fig. S2A and B).

Pathological changes in pulmonary vessels in mice exposed to hypoxia for four weeks

Since the degree of the PH phenotype did not differ between mice under hypoxia for four and 12 weeks, we performed pathological analysis of the lungs using mice exposed to hypoxia for four weeks. Immunostaining of mouse lungs for αSMA showed that the number of muscularized pulmonary vessels in mice exposed to hypoxia was significantly higher in EC-Mut Tg mice than in EC-WT Tg, KO, and WT mice (Fig. 3a, b). However, there were no differences in the thickness of the pulmonary vessel wall among the mice

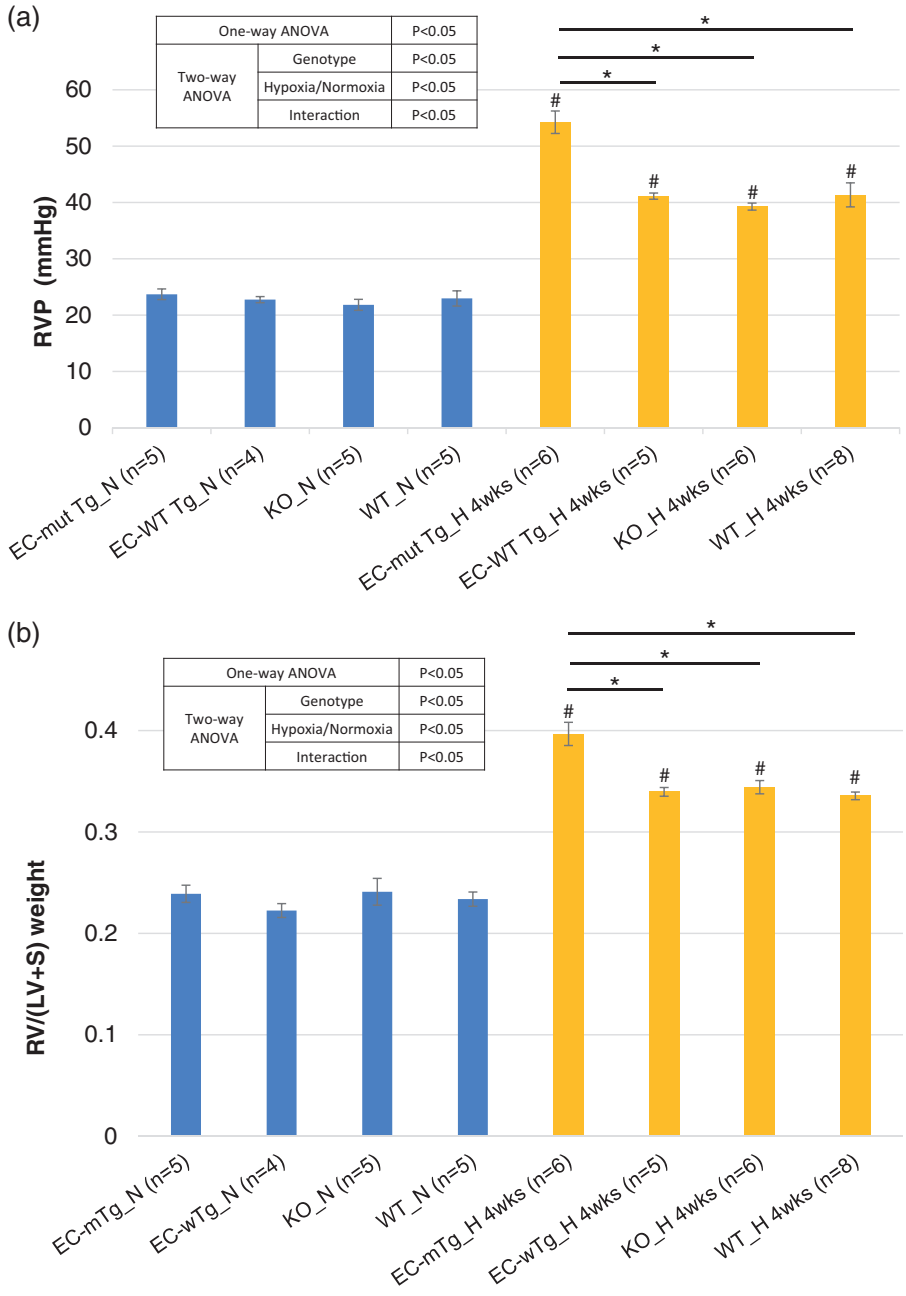

Fig. 2. Physiological PH phenotypes of EC-Mut Tg, EC-WT Tg, KO, and WT mice exposed to hypoxia. (a) RVP and (b) RV/(LV + S) of EC-Mut Tg, EC-WT Tg, KO, and WT mice under conditions of normoxia (N) and hypoxia for four weeks (H_4wks). Data with bars represent mean ± SEM. The number of experiments (n) is indicated in each figure. There were significant differences ($P < 0.05$) in the values of RVP and RV/(LV + S) among the eight groups (grouped by genotype and normoxia/hypoxia) using one-way ANOVA. *$P < 0.05$, by Tukey's post-hoc test compared with EC-Mut Tg mice. #$P < 0.05$, by Tukey's post-hoc test compared with normoxia.

genotypes or under the different oxygen conditions (Fig. 3C). Two-way ANOVA demonstrated that genotypes, hypoxia, and their interaction were significant for vessel number, whereas none of these factors was significant for vessel thickness (Fig. 3b, c). These results demonstrate that EC-specific *Rnf213* mutant overexpression enhances pulmonary artery muscularization in chronic hypoxic mice, which is consistent with the PH physiological data. Furthermore, electron microscopy showed characteristic EC detachment from the basement membrane in pulmonary vessels of EC-Mut Tg mice under hypoxia, whereas such detachment was not observed in EC-WT Tg, KO, or WT mice under hypoxia, or in EC-Mut Tg mice under normoxia (Fig. 4). Interestingly, such EC detachment in pulmonary

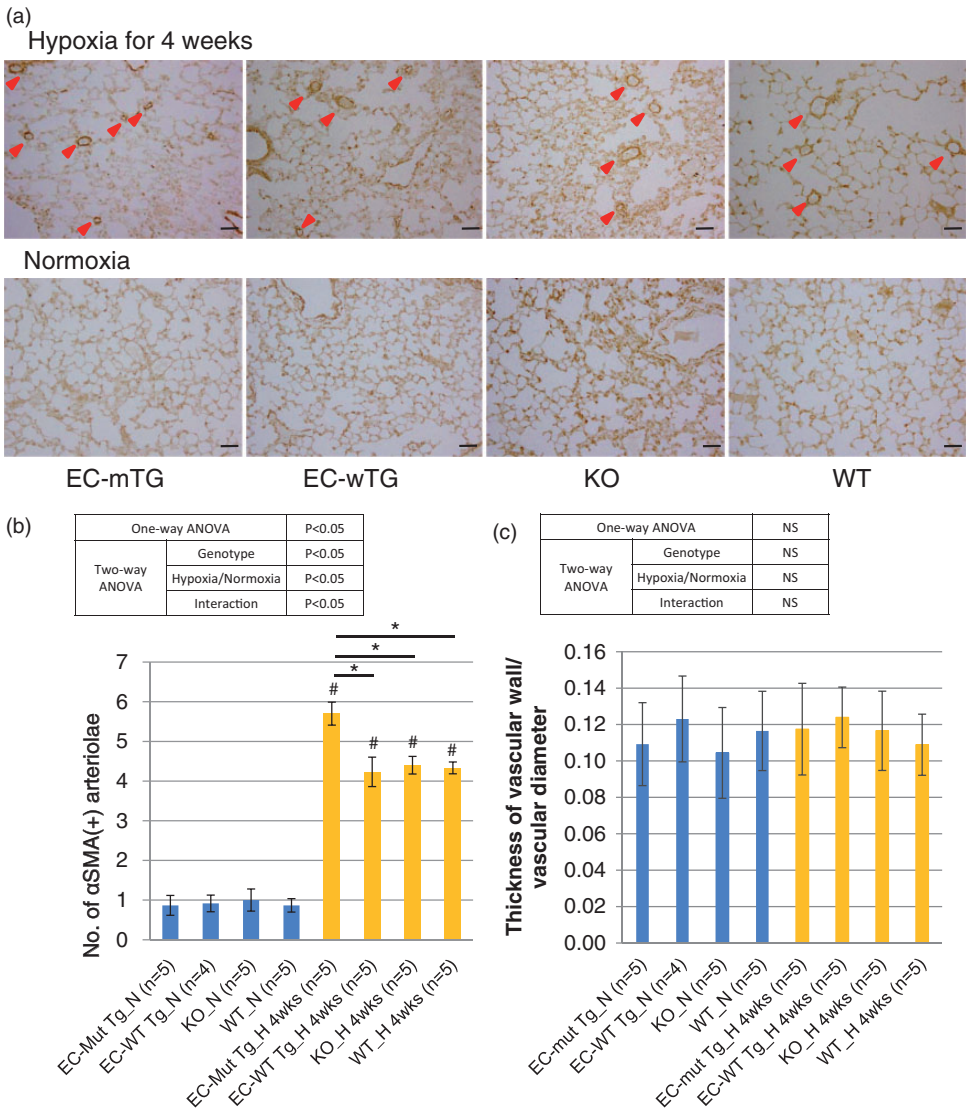

Fig. 3. Histopathological changes in pulmonary vessels in EC-Mut Tg, EC-WT Tg, KO, and WT mice exposed to hypoxia. (a) Representative images of αSMA-stained sections of the lungs of EC-Mut Tg, EC-WT Tg, KO, and WT mice under normoxia and hypoxia for four weeks. Red arrowheads indicate αSMA-positive (muscularized) vessels. Scale bars indicate 50 μm. (b, c) Quantified results of (b) the number and (c) thickness of αSMA-positive pulmonary vessels in EC-Mut Tg, EC-WT Tg, KO, and WT mice under conditions of normoxia (N) and hypoxia for four weeks (H_4wks). Data with bars represent mean ± SEM. The number of experiments (n) is indicated in each figure. There were significant differences ($P < 0.05$) in the number, but not in the thickness, of vessels among the eight groups (grouped by genotype and normoxia/hypoxia) using one-way ANOVA. *$P < 0.05$, by Tukey's post-hoc test compared with EC-Mut Tg mice. #$P < 0.05$, by Tukey's post-hoc test compared with normoxia. NS, not significant.

arteries is similar to the phenotypes observed in model mice lacking Cav-1, a key molecule involved in EC function.[39]

Cav-1 in lungs of mice exposed to hypoxia for one and four weeks

To evaluate Cav-1 levels in pulmonary vascular ECs of EC-Mut Tg under hypoxia, immunohistochemistry and western blotting for Cav-1 were performed using mouse lungs. Immunohistochemistry data showed strong staining intensity in pulmonary vascular ECs in EC-Mut Tg, KO, and WT mice under both normoxia and hypoxia for four weeks (Fig. 5a), suggesting that Cav-1 levels in lung tissue reflect the levels in vascular ECs. We also compared the Cav-1 levels in EC-Mut Tg, WT, and KO mice exposed to hypoxia for one or four weeks by western blot analysis. The hypoxia mouse model used in the present study was reported to start displaying changes in gene expression profiles in pulmonary arteries one week after hypoxia exposure.[40] Although Cav-1 levels decreased in all genotypes

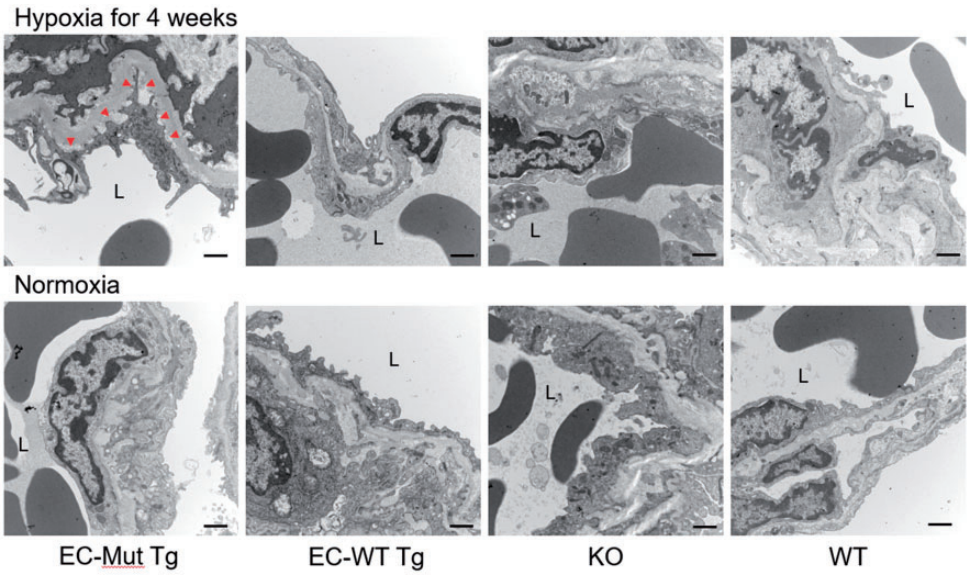

Fig. 4. Electron microscopy of pulmonary vessels in EC-Mut Tg, EC-WT Tg, KO, and WT mice exposed to hypoxia. Representative electron micrographs of pulmonary vessels of EC-Mut Tg, EC-WT Tg, KO, and WT mice under normoxia or hypoxia for four weeks. Red arrowheads show areas of EC detachment from the basement membrane. "L" indicates the lumen of vessels. Scale bars indicate 2 μm.

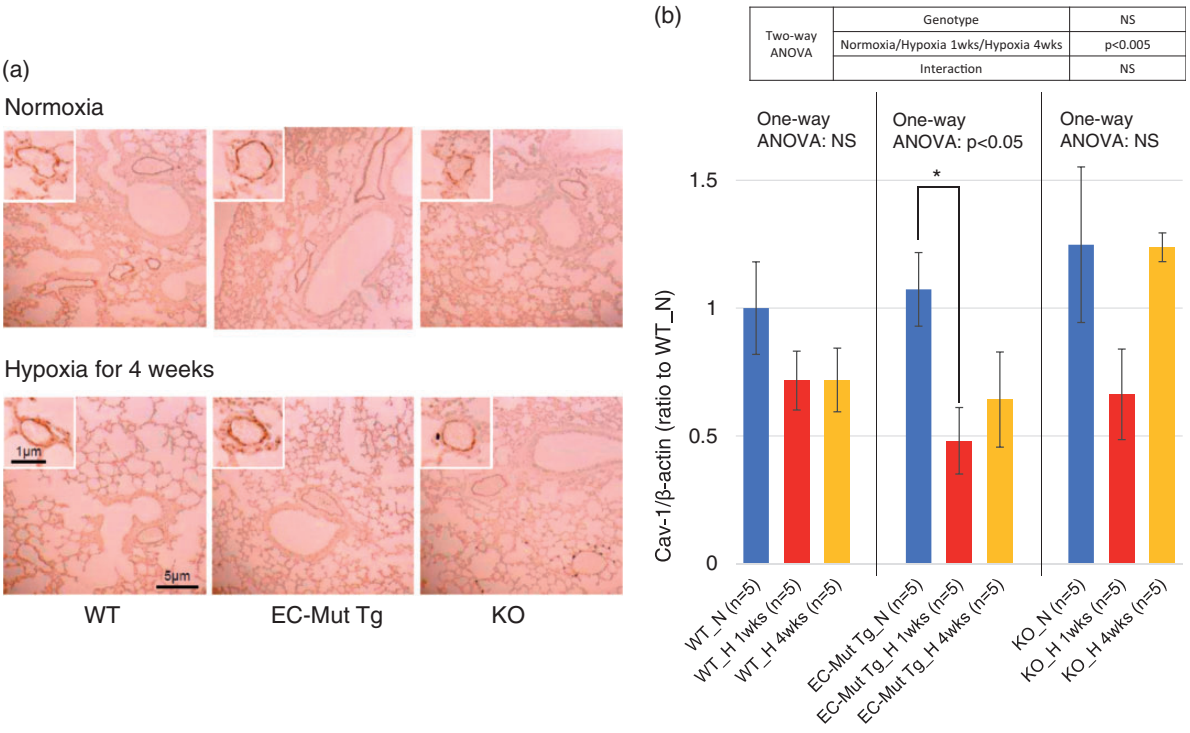

Fig. 5. Cav-1 expression in lungs of EC-Mut Tg, KO, and WT mice exposed to hypoxia. (a) Representative images o.f lung immunohistochemistry for Cav-1 in EC-Mut Tg, KO, and WT mice under normoxia or hypoxia for four weeks. Similar results were obtained from three independent experiments. The small boxes showCav-1 immunostaining in pulmonary vascular ECs. The scale bars represent the indicated dimensions.
(b) Quantified data of western blotting for Cav-1 levels in lungs of EC-Mut Tg, KO, and WT mice under normoxia (N), hypoxia for one week (H 1wks) and hypoxia for four weeks (H 4wks). Western blot images are shown in Fig. S3. β-actin was used as internal control. The values are relative intensities normalized to WT mice under normoxia (WT_N). Data with bars represent mean ± SEM. The number of experiments (n) is indicated in the figure. There were no significant differences among WT_N, EC-Mut Tg_N and KO_N by one-way ANOVA ($P > 0.05$). One-way ANOVA comparing Cav-1 levels among normoxia, hypoxia for one week and hypoxia for four weeks in each genotype shows that there were significant differences ($P < 0.05$) in EC-Mut Tg mice, but not in WT and KO mice. *$P < 0.05$, by Tukey's post-hoc test compared with normoxia. NS, not significant.

after one week of hypoxia, the reductions in comparison with normoxic conditions were only significant in EC-Mut Tg mice, but not in WT or KO mice (Fig. 5b and Fig. S3).

Histology of cerebral blood vessels in mice exposed to hypoxia for 12 weeks

To examine the effect of *RNF213* variants on cerebral blood vessels, we estimated the extent of hypoxia-induced angiogenesis and stenotic vascular change in the cerebrum of EC-Mut Tg and WT mice exposed to long-term (12 weeks) hypoxia. Under long-term hypoxia, EC-Mut Tg mice possessed a significantly smaller number of cerebral microvessels than WT mice (Fig. S2C). However, there were no differences in cerebrovascular wall thickness between the EC-Mut Tg and WT mice (Fig. S2D). These results suggest that although MMD-associated *RNF213* variants inhibit angiogenesis via EC dysfunction, this does not lead to stenotic changes in cerebral blood vessels. These findings are consistent with the results of our previous mouse model study under short-term hypoxia.[29]

Discussion

Our clinical case study showed that rare variants (including p.R4810K) in the C-terminal region of *RNF213* were present in some Japanese patients who suffered from PH. This observed association of p.R4810K with PH was confirmed by an exaggerated PH phenotype in *Rnf213* p.R4757K Tg mice after exposure to hypoxia. These findings suggest that deleterious *RNF213* variants, such as p.R4810K, could be risk factors for PH.

Of the 27 patients with PH, disease-associated variants in the C-terminus of *RNF213* were observed in 7.4% (2/27) of patients. Three non-synonymous *BMPR2* variants (p.Q92H, p.L198Rfs*4, and p.S930X) were found in three of the 27 (11.1%) patients. No patient harbored both *RNF213* and *BMPR2* variants. These results suggest that *RNF213* variants contribute to some proportion of Japanese PH patients independently of *BMPR2* variants.

The present study using a hypoxia-induced PH mouse model demonstrates that the PH parameters of WT, EC-WT Tg, EC-Mut Tg, and KO mice did not differ under normoxia, whereas the EC-Mut Tg mice showed exacerbated PH parameters under hypoxia compared with the other genotypes. The manifestation of these aggravated PH phenotypes in the EC-Mut Tg but not in KO mice imply that the *RNF213* mutant reduces angiogenesis through a gain-of-function mechanism in the lung as well as in the brain. This concept is supported by our previous in vitro study[30] demonstrating that overexpression of the *RNF213* mutant, but not *RNF213* suppression by RNAi, inhibited angiogenesis in EC cell models. These results provide two important insights into the *RNF213* mutant: first, that they mainly play a role in vascular EC functions; and second, that may have deleterious effects under stress conditions, such as hypoxia, but not under normal conditions, in vivo.

Reduced angiogenesis, which reflects EC dysfunction induced by *RNF213* mutants, has been reported by our cellular biology and animal studies.[29,30,41] Angiogenesis was reduced in ECs differentiated from iPS cells of MMD patients with *RNF213* p.R4810K, as well as in cultured ECs overexpressing *RNF213* p.R4810K.[30] Reduced angiogenesis in ECs has also been reported by overexpression of other MMD-associated *RNF213* mutants.[41] Additionally, hypoxia-induced angiogenesis in the brain is found to be inhibited in EC-Mut Tg mice,[29] as also confirmed in the present study.

In the present study, electron microscopy showed characteristic EC detachment from the basement membrane in pulmonary arteries of EC-Mut Tg mice under hypoxia, similar to that observed in pulmonary arteries of Cav-1 KO mice.[39] Surprisingly, Cav-1 reduction was observed in the lungs of EC-Mut Tg mice in comparison with WT and KO mice. Cav-1 is a major protein constituent of caveolae and regulates EC function via interactions with several signaling molecules.[42,43] Several studies have suggested that Cav-1 deficiency may lead to PH: a heterozygous frameshift mutation in the Cav-1 gene was identified as a cause of familial PH;[17] Cav-1 KO mice were found to exhibit PH;[15] reduced Cav-1 protein was observed in ECs from pulmonary arteries of PH patients;[44] and low serum Cav-1 levels were observed in patients with PH[45] as well as MMD.[46] These findings raise the possibility that Cav-1 suppression plays a role in the *RNF213* mutant-associated PH aggravation, although at present its causality remains unclear.

In the present study, mutant *Rnf213* overexpression in ECs resulted in a significant aggravation of the PH phenotype, but only under hypoxia. Genetic epidemiological studies on MMD have shown that the penetrance of *RNF213* p.R4810K is low (1/200 carriers), although it is strongly associated with the disease (odds ratio > 100) in East Asians.[25] Interestingly, *BMPR2* variants also show such incomplete penetrance (approximately 20%) in PH.[12] These reports suggest that environmental factors may be required to trigger the inherited susceptibility in patients with PH and MMD.

Although the environmental factors linked with *RNF213* mutants remain largely unknown, several in vitro studies have provided some clues. Recently, Banh et al.[27] reported that *RNF213* was an essential mediator of non-mitochondrial oxygen consumption by PTP1B in Her2+ breast cancer cells.[27] They suggested that activation of *RNF213*, which is negatively regulated by PTP1B, induces a reduction in oxygen availability and results in hypoxia-induced cell death.[27] Therefore, *RNF213* mutants may cause vascular ECs to become more susceptible to hypoxia, leading to EC dysfunction, cell death, and subsequent vascular stenotic change. In addition, recent reports have shown *RNF213* upregulation in ECs by interferons,[28,29] suggesting the involvement of inflammatory signals in *RNF213*-induced EC dysfunction.

In this study, *RNF213* variants were found less frequently (7.4%) in Japanese cases of PH than in Japanese cases of MMD (approximately 90%). This finding suggests that cerebral arteries (MMD) are far more susceptible to *RNF213* variants than pulmonary arteries (PH) in humans. In contrast, in the mouse model exposed to hypoxia, *RNF213* mutant overexpression in ECs led to stenotic pathological changes, such as aggravated muscularization in the pulmonary artery, but not in cerebral arteries. Such discordance may be explained by species differences and/or the tissue types. There are clearly interspecies differences in pulmonary artery remodeling response to PH-promoting stimuli.[47] Therefore, the susceptibility of SMCs is most likely considered to be dependent on species. However, it should be noted that overexpression of the *RNF213* mutation in EC is enough to aggravate PH after hypoxia exposure, which is known to be mediated by a reduced potential for adaptive angiogenesis,[14,18] being consistent with confirmed lowered adaptive angiogenesis in brain.

Relatively small patient population size is a limitation of this study. Here, the detection rate of the *BMPR2* mutation (11.1%) in PH patients was lower than that in two previous studies of Japanese PH cases (30–40% in sporadic PH cases).[37,38] Although this inconsistency between studies could be explained by the fact that, in the present study we included secondary PH cases, and our screening strategy did not target large exonic deletions/insertions, we cannot completely exclude the possibility that such a small population size limits more general conclusions. Further large-scale studies to confirm the association of *RNF213* variants with PH are required. The use of lung tissue to evaluate Cav-1 levels is one other limitation, as our primary focus was on Cav-1 expression in vascular ECs. However, a number of studies using lung tissues have successfully demonstrated the effects of treatment via Cav-1 on PH in animal models,[48–50] indicating that lung tissue use may be sensitive enough to detect vascular changes in Cav-1. Another limitation of the present study is in regard to the tissue-specificity of gene overexpression by the Tie2 promoter-driven Cre system in the Tg mice. Despite the common use of this Tg system for specific overexpression in ECs, it also leads to overexpression in hematopoietic Tie2-expressing cells,[51] potentially complicating the interpretation of the phenotype of the EC-Mut Tg mice. Although our previous cell model studies,[29,30,41] which demonstrated the deleterious effects of *RNF213* mutants on ECs, suggest that the observed phenotype is primarily related to *RNF213* mutant overexpression in ECs, further studies using animal models overexpressing *RNF213* mutants specifically in hematopoietic cells are required to clarify the roles of *RNF213* mutants in hematopoietic cells.

In conclusion, the present genetic and animal model data suggest that *RNF213*, a susceptibility gene for MMD, is one of the genes associated with PH. *RNF213* variants have also been associated with other vascular diseases, such as coronary artery disease,[7] and high systolic blood pressure.[8] These findings strongly suggest that *RNF213* plays a role in systemic vasculopathy. Future genetic epidemiological and biomedical studies are required to investigate the associations between *RNF213* and various vascular diseases.

Conflict of interest

The author(s) declare that there is no conflict of interest.

Funding

This work was supported by a Grant-in-Aid of Scientific Research on Innovative Areas to A. Koizumi (JP17H06397) and a grant from the Research Committee on Spontaneous Occlusion of the Circle of Willis of the Ministry of Health and Welfare of Japan (No. H26-Nanjito-Ippan-078).

References

1. Liu W, Morito D, Takashima S, et al. Identification of RNF213 as a susceptibility gene for moyamoya disease and its possible role in vascular development. *PLoS One* 2011; 6: e22542.
2. Kamada F, Aoki Y, Narisawa A, et al. A genome-wide association study identifies RNF213 as the first Moyamoya disease gene. *J Hum Genet* 2011; 56: 34–40.
3. Kudo T. Spontaneous occlusion of the circle of Willis. A disease apparently confined to Japanese. *Neurology* 1968; 18: 485–496.
4. Suzuki J and Takaku A. Cerebrovascular "moyamoya" disease. Disease showing abnormal net-like vessels in base of brain. *Arch Neurol* 1969; 20: 288–299.
5. Takeuchi K and Shimizu K. Hypoplasia of bilateral internal carotid arteries (in Japanese). *Brain Nerve* 1957; 9: 37–43.
6. Ikeda E. Systemic vascular changes in spontaneous occlusion of the circle of Willis. *Stroke* 1991; 22: 1358–1362.
7. Morimoto T, Mineharu Y, Ono K, et al. Significant association of RNF213 p.R4810K, a moyamoya susceptibility variant, with coronary artery disease. *PLoS One* 2017; 12: e0175649.
8. Koizumi A, Kobayashi H, Liu W, et al. P.R4810K, a polymorphism of RNF213, the susceptibility gene for moyamoya disease, is associated with blood pressure. *Environ Health Prev Med* 2013; 18: 121–129.
9. Galie N, Humbert M, Vachiery JL, et al. 2015 ESC/ERS Guidelines for the diagnosis and treatment of pulmonary hypertension: The Joint Task Force for the Diagnosis and Treatment of Pulmonary Hypertension of the European Society of Cardiology (ESC) and the European Respiratory Society (ERS): Endorsed by: Association for European Paediatric and Congenital Cardiology (AEPC), International Society for Heart and Lung Transplantation (ISHLT). *Eur Heart J* 2016; 37: 67–119.
10. Deng Z, Morse JH, Slager SL, et al. Familial primary pulmonary hypertension (gene PPH1) is caused by mutations in the bone morphogenetic protein receptor-II gene. *Am J Hum Genet* 2000; 67: 737–744.
11. International PPH Consortium, Lane KB, Machado RD, et al. Heterozygous germline mutations in BMPR2, encoding a TGF-beta receptor, cause familial primary pulmonary hypertension. *Nat Genet* 2000; 26: 81–84.

12. Ma L and Chung WK. The role of genetics in pulmonary arterial hypertension. *J Pathol* 2017; 241: 273–280.
13. Austin ED, Loyd JE and Phillips JA III. Heritable pulmonary arterial hypertension. *GeneReviews®*. Available at: https://www.ncbi.nlm.nih.gov/books/NBK1485/ (accessed 10 Nov 2017).
14. Ranchoux B, Harvey LD, Ayon RJ, et al. Endothelial dysfunction in pulmonary arterial hypertension: an evolving landscape (2017 Grover Conference Series). *Pulm Circ* 2018; 8: 2045893217752912.
15. Zhao YY, Liu Y, Stan RV, et al. Defects in caveolin-1 cause dilated cardiomyopathy and pulmonary hypertension in knockout mice. *Proc Natl Acad Sci U S A* 2002; 99: 11375–11380.
16. Asosingh K, Farha S, Lichtin A, et al. Pulmonary vascular disease in mice xenografted with human BM progenitors from patients with pulmonary arterial hypertension. *Blood* 2012; 120: 1218–1227.
17. Austin ED, Ma L, LeDuc C, et al. Whole exome sequencing to identify a novel gene (caveolin-1) associated with human pulmonary arterial hypertension. *Circ Cardiovasc Genet* 2012; 5: 336–343.
18. Nickel NP, Spiekerkoetter E, Gu M, et al. Elafin reverses pulmonary hypertension via caveolin-1-dependent bone morphogenetic protein signaling. *Am J Respir Crit Care Med* 2015; 191: 1273–1286.
19. Fukushima H, Takenouchi T and Kosaki K. Homozygosity for moyamoya disease risk allele leads to moyamoya disease with extracranial systemic and pulmonary vasculopathy. *Am J Med Genet A* 2016; 170: 2453–2456.
20. Kapusta L, Daniels O and Renier WO. Moya-Moya syndrome and primary pulmonary hypertension in childhood. *Neuropediatrics* 1990; 21: 162–163.
21. Ou P, Dupont P and Bonnet D. Fibromuscular dysplasia as the substrate for systemic and pulmonary hypertension in the setting of Moya-Moya disease. *Cardiol Young* 2006; 16: 495–497.
22. Tokunaga K, Hishikawa T, Sugiu K, et al. Fatal outcomes of pediatric patients with moyamoya disease associated with pulmonary arterial hypertension. Report of two cases. *Clin Neurol Neurosurg* 2013; 115: 335–338.
23. Chang SA, Song JS, Park TK, et al. Nonsyndromic peripheral pulmonary artery stenosis is associated with homozygosity of RNF213 p.Arg4810Lys regardless of co-occurrence of Moyamoya disease. *Chest* 2018; 153: 404–413.
24. Morito D, Nishikawa K, Hoseki J, et al. Moyamoya disease-associated protein mysterin/RNF213 is a novel AAA+ ATPase, which dynamically changes its oligomeric state. *Sci Rep* 2014; 4: 4442.
25. Koizumi A, Kobayashi H, Hitomi T, et al. A new horizon of moyamoya disease and associated health risks explored through RNF213. *Environ Health Prev Med* 2016; 21: 55–70.
26. Scholz B, Korn C, Wojtarowicz J, et al. Endothelial RSPO3 controls vascular stability and pruning through non-canonical WNT/Ca(2+)/NFAT signaling. *Dev Cell* 2016; 36: 79–93.
27. Banh RS, Iorio C, Marcotte R, et al. PTP1B controls non-mitochondrial oxygen consumption by regulating RNF213 to promote tumour survival during hypoxia. *Nat Cell Biol* 2016; 18: 803–813.
28. Ohkubo K, Sakai Y, Inoue H, et al. Moyamoya disease susceptibility gene RNF213 links inflammatory and angiogenic signals in endothelial cells. *Sci Rep* 2015; 5: 13191.
29. Kobayashi H, Matsuda Y, Hitomi T, et al. Biochemical and functional characterization of RNF213 (Mysterin) R4810K, a susceptibility mutation of moyamoya disease, in angiogenesis in vitro and in vivo. *J Am Heart Assoc* 2015; 4: e002146.
30. Hitomi T, Habu T, Kobayashi H, et al. Downregulation of Securin by the variant RNF213 R4810K (rs112735431, G > A) reduces angiogenic activity of induced pluripotent stem cell-derived vascular endothelial cells from moyamoya patients. *Biochem Biophys Res Commun* 2013; 438: 13–19.
31. Austin ED and Loyd JE. The genetics of pulmonary arterial hypertension. *Circ Res* 2014; 115: 189–202. 2014/06/22. DOI: 10.1161/CIRCRESAHA.115.303404.
32. McDonald J, Wooderchak-Donahue W, VanSant Webb C, et al. Hereditary hemorrhagic telangiectasia: genetics and molecular diagnostics in a new era. *Front Genet* 2015; 6: 1.
33. Dakeishi M, Shioya T, Wada Y, et al. Genetic epidemiology of hereditary hemorrhagic telangiectasia in a local community in the northern part of Japan. *Hum Mutat* 2002; 19: 140–148.
34. Kobayashi H, Yamazaki S, Takashima S, et al. Ablation of Rnf213 retards progression of diabetes in the Akita mouse. *Biochem Biophys Res Commun* 2013; 432: 519–525.
35. Zhao L, Mason NA, Morrell NW, et al. Sildenafil inhibits hypoxia-induced pulmonary hypertension. *Circulation* 2001; 104: 424–428.
36. Wu Z, Jiang H, Zhang L, et al. Molecular analysis of RNF213 gene for moyamoya disease in the Chinese Han population. *PLoS One* 2012; 7: e48179.
37. Kabata H, Satoh T, Kataoka M, et al. Bone morphogenetic protein receptor type 2 mutations, clinical phenotypes and outcomes of Japanese patients with sporadic or familial pulmonary hypertension. *Respirology* 2013; 18: 1076–1082.
38. Morisaki H, Nakanishi N, Kyotani S, et al. BMPR2 mutations found in Japanese patients with familial and sporadic primary pulmonary hypertension. *Hum Mutat* 2004; 23: 632.
39. Schubert W, Frank PG, Woodman SE, et al. Microvascular hyperpermeability in caveolin-1 (-/-) knock-out mice. Treatment with a specific nitric-oxide synthase inhibitor, L-NAME, restores normal microvascular permeability in Cav-1 null mice. *J Biol Chem* 2002; 277: 40091–40098.
40. Kwapiszewska G, Wilhelm J, Wolff S, et al. Expression profiling of laser-microdissected intrapulmonary arteries in hypoxia-induced pulmonary hypertension. *Respir Res* 2005; 6: 109.
41. Kobayashi H, Brozman M, Kyselova K, et al. RNF213 rare variants in Slovakian and Czech moyamoya disease patients. *PLoS One* 2016; 11: e0164759.
42. Mathew R. Pathogenesis of pulmonary hypertension: a case for caveolin-1 and cell membrane integrity. *Am J Physiol Heart Circ Physiol* 2014; 306: H15–25.
43. Minshall RD, Sessa WC, Stan RV, et al. Caveolin regulation of endothelial function. *Am J Physiol Lung Cell Mol Physiol* 2003; 285: L1179–1183.
44. Bakhshi FR, Mao M, Shajahan AN, et al. Nitrosation-dependent caveolin 1 phosphorylation, ubiquitination, and degradation and its association with idiopathic pulmonary arterial hypertension. *Pulm Circ* 2013; 3: 816–830.
45. Wang KY, Lee MF, Ho HC, et al. Serum caveolin-1 as a novel biomarker in idiopathic pulmonary artery hypertension. *Biomed Res Int* 2015; 2015: 173970.

46. Bang OY, Chung JW, Kim SJ, et al. Caveolin-1, Ring finger protein 213, and endothelial function in Moyamoya disease. *Int J Stroke* 2016; 11: 999–1008.
47. Stenmark KR, Meyrick B, Galie N, et al. Animal models of pulmonary arterial hypertension: the hope for etiological discovery and pharmacological cure. *Am J Physiol Lung Cell Mol Physiol* 2009; 297: L1013–1032.
48. Bauer PM, Bauer EM, Rogers NM, et al. Activated CD47 promotes pulmonary arterial hypertension through targeting caveolin-1. *Cardiovasc Res* 2012; 93: 682–693.
49. Tian J, Smith A, Nechtman J, et al. Effect of PPARgamma inhibition on pulmonary endothelial cell gene expression: gene profiling in pulmonary hypertension. *Physiol Genomics* 2009; 40: 48–60.
50. Zhang HL, Liu ZH, Luo Q, et al. Abnormal expression of NSF, alpha-SNAP and SNAP23 in pulmonary arterial hypertension in rats treated with monocrotaline. *Int J Clin Exp Med* 2015; 8: 1834–1843.
51. Oladipupo SS, Smith C, Santeford A, et al. Endothelial cell FGF signaling is required for injury response but not for vascular homeostasis. *Proc Natl Acad Sci U S A* 2014; 111: 13379–13384.